IJMMM International Journal of Minerals, Metallurgy and Materials 矿物冶金与材料学报（英文版）

Role of tannin pretreatment in flotation separation of magnesite and dolomite

Xiufeng Gong, Jin Yao, Jun Guo, Bin Yang, Haoran Sun, Wanzhong Yin, Yulian Wang, and Yafeng Fu

Cite this article as:
Xiufeng Gong, Jin Yao, Jun Guo, Bin Yang, Haoran Sun, Wanzhong Yin, Yulian Wang, and Yafeng Fu, Role of tannin pretreatment in flotation separation of magnesite and dolomite, *Int. J. Miner. Metall. Mater.*, 31(2024), No. 3, pp. 452-461. https://doi.org/10.1007/s12613-023-2708-4

View the article online at SpringerLink or IJMMM Webpage.

INTERNATIONAL JOURNAL OF
Minerals, Metallurgy and Materials

Volume 31, Number 3, March 2024
Page 452

Research Article https://doi.org/10.1007/s12613-023-2708-4

Role of tannin pretreatment in flotation separation of magnesite and dolomite

Xiufeng Gong[1)], *Jin Yao*[1,2),✉], *Jun Guo*[1)], *Bin Yang*[3),✉], *Haoran Sun*[4)], *Wanzhong Yin*[1)], *Yulian Wang*[4),✉], *and Yafeng Fu*[5)]

1) School of Resources and Civil Engineering, Northeastern University, Shenyang 110819, China
2) Key Laboratory of Solid Waste Treatment and Resource Utilization of the Ministry of Education, Southwest University of Science and Technology, Mianyang 621010, China
3) School of Chemical Engineering, China University of Mining and Technology, Xuzhou 221116, China
4) School of Materials Science and Engineering, Shenyang Ligong University, Shenyang 110159, China
5) Ansteel Beijing Research Institute Co., Ltd., Beijing 102200, China
(Received: 21 March 2023; revised: 9 July 2023; accepted: 11 July 2023)

Abstract: Flotation separation of magnesite and its calcium-containing carbonate minerals is a difficult problem. Recently, new regulators have been proposed for magnesite flotation decalcification, although traditional regulators such as tannin, water glass, sodium carbonate, and sodium hexametaphosphate are more widely used in industry. However, they are rarely used as the main regulators in research because they perform poorly in magnesite and dolomite single-mineral flotation tests. Inspired by the limonite presedimentation method and the addition of a regulator to magnesite slurry mixing, we used a tannin pretreatment method for separating magnesite and dolomite. Microflotation experiments confirmed that the tannin pretreatment method selectively and largely reduces the flotation recovery rate of dolomite without affecting the flotation recovery rate of magnesite. Moreover, the contact angles of the tannin-pretreated magnesite and dolomite increased and decreased, respectively, in the presence of NaOl. Zeta potential and Fourier transform infrared analyses showed that the tannin pretreatment method efficiently hinders NaOl adsorption on the dolomite surface but does not affect NaOl adsorption on the magnesite surface. X-ray photoelectron spectroscopy and density functional theory calculations confirmed that tannin interacts more strongly with dolomite than with magnesite.

Keywords: tannin pretreatment; selective inhibition; flotation separation; magnesite; dolomite

1. Introduction

Magnesite is a primary source of metallic magnesium, which is widely used in building materials, refractories, chemical materials, and adhesive materials [1–2]. Magnesite is a magnesium carbonate mineral usually found in sedimentary rocks with organic components, most of which are stratified or nodular. Such rocks are often associated with calcium-bearing minerals [3–5]. The commonest calcium-bearing gangue minerals in magnesite is dolomite, an essential component in the ceramics, glass, agriculture, environmental protection, and other industries [6]. By separating magnesite from dolomite, we could fully utilize both the target mineral (magnesite) and the gangue mineral (dolomite) [7].

Foam flotation is a mineral separation method that is more widely used than gravity separation, magnetic separation, electrostatic separation, and chemical separation [8–10]. This method fully utilizes the differences in surface properties between target minerals and gangue minerals, and can achieve higher concentrate grades and flotation recovery rates [11–12]. At the same time, foam flotation can successfully solve the problem of difficult separation of alkaline earth metal minerals such as magnesite and dolomite due to similar active atomic spacing, mineral composition, and adsorption mechanism [13–15].

When separating magnesite from its ore, one must first select the collector. Highly selective long-chain collectors exert a strong collection effect; therefore, fatty acids and dodecylamine are often used in flotation tests [16–18]. The selected regulator crucially determines the success of the separation. Although fatty acid collectors are suitable for positive flotation separation, an amine collector can be adopted in reverse flotation separation [19–22]. To separate magnesite and dolomite using the reverse flotation method, Yao *et al.* [18] applied the regulator sodium dihydrogen phosphate (SDP), which selectively adsorbs to the dolomite surface. Zhu *et al.* [21] found that carboxymethyl cellulose exerts a strong adsorption effect on magnesite but is an ineffective regulator on quartz. The selective collection of quartz by dodecylamine (DDA) achieves flotation separation of the two minerals. Sun *et al.* [23] demonstrated that adding the chelating agent ethyl-

✉ Corresponding authors: Jin Yao E-mail: yaojin@mail.neu.edu.cn; Bin Yang E-mail: nemoybmaster@outlook.com; Yulian Wang E-mail: ylwang0908@163.com

enediamine tetra (methylene phosphonic acid) sodium (EDTMPS) prior to the flotation test selectively inhibits magnesite in a DDA flotation system. Using oleate as the collector and 1-hydroxyethylene-1,1diphosphonic acid (HEDP) as the regulator, Yang *et al.* [24] found that HEDP obviously inhibits dolomite and achieves positive flotation separation of magnesite and dolomite. A regulator is a crucial component in the flotation separation of minerals. A commonly used regulator can reduce the cost and expand the application range of the agent [25–27].

Tannic acid is a weakly acidic, high-molecular-weight polyphenol derived from plants and trees [28]. As a common organic regulator, tannic acid has attracted much attention in various fields [17]. The structure of tannic acid is shown in Fig. S1. Owing to its numerous adjacent hydroxyl groups, tannic acid has a strong affinity for metal ions and inhibits metal minerals [25,29]. Studies on tannic-acid flotation have reported that larch tannin extract improves jamesonite flotation and that quebracho affects the flotation separation of scheelite and calcite, celestite and calcite, and fluorite and calcite [25,30–32]. All of these studies have laid a solid foundation for investigating the decalcification of tannic acid.

Previously, we showed that when sodium oleate (NaOl) is used as a collector, magnesite and dolomite have similar floatabilities and cannot be separated without regulators [20,33–34]. This study examines the performance of the tannin pretreatment method during flotation separation of magnesite and dolomite in a NaOl system. The pure magnesite and dolomite minerals are pretreated with tannin regulator before the flotation test. The flotation test of the pretreated mineral samples is the highlight of this study. Some studies have shown that pretreatment changes the mineral properties such as wettability and charge on the mineral surface, thereby improving the mineral floatability. Considering the excellent properties of tannin, we selected tannin as the modifier in magnesite and dolomite separation. However, flotation tests of single magnesite and dolomite minerals indicated that tannin inhibits the flotation of magnesite and dolomite; moreover, the flotations of the two minerals are only slightly different. To avoid these problems, we added EDTMPS to the stirred slurry before the flotation test and exploited the previously reported favorable effect of presedimentation in limonite flotation. Combined with the pretreatment method, we learned that EDTMPS addition preferentially changes the mineral properties such as wettability and the mineral surface charge [23,35–37]. Therefore, this study proposes the pretreatment of magnesite and dolomite monominerals with tannin in the NaOl flotation system. The feasibility of this method was verified through flotation tests on the pretreated minerals. After confirming good flotation results of the tannin pretreatment method, we investigated the reasons for the effective magnesite and dolomite flotation separation through contact angle measurements, zeta potential determination, Fourier transform infrared spectroscopy (FT-IR), X-ray photoelectron spectroscopy (XPS) detection, and density functional theory (DFT) simulations.

2. Experimental

2.1. Materials and reagents

The test materials were pure minerals of magnesite and dolomite sourced from Dashiqiao, Yingkou (Liaoning, China). Fig. S2 shows the X-ray diffraction (XRD) spectra of magnesite and dolomite and Table S1 shows their chemical compositions determined via X-ray fluorescence chemical analysis. The purities of magnesite and dolomite were 98.56% (by MgO) and 98.42% (by CaO), respectively [38]. Before the test, a single mineral was prepared via crushing, hand sorting, grinding, screening, and other processing methods. The ore sample (particle size = −74+38 μm) was selected as the flotation feed. NaOl was purchased as a pure chemical reagent from Sinopharm Group Chemical Reagent Co., Ltd. (Liaoning, China) and pure tannin was purchased from Tianjin Kemi Ou Chemical Reagent Co., Ltd. (Liaoning, China). The pH of the pulp was adjusted using HCl and NaOH. All tests were performed in deionized water.

2.2. Tannin pretreatment process

For the tannin pretreatment process, 100 g of the mineral (magnesite or dolomite) and 400 mL of tannin solution were added to a 500-mL beaker. After stirring for 5 min with a magnetic agitator, the pretreated ore sample was washed five times with deionized water to remove tannin liquid from the surface of the mineral particles. The pulp was passed through a vacuum filter and the resulting filter cake was dried at room temperature and used as the flotation feed; subsequently, the filtrate was discarded. Fig. S3 is a flowchart of the tannin pretreatment process.

2.3. Microflotation test

Flotation tests were performed in an XFG-ii hanging-trough flotation machine (Jilin Prospecting Machinery Factory) operated at 1992 r/min [39]. For each test, 2.0 g of the ore sample was placed in the 30-mL flotation tank and 20 mL of deionized water was added. After stirring for 2 min, the pH of the pulp was adjusted with HCl or NaOH and the pulp was stirred further for 3 min. Next, NaOl was added and the pulp was stirred for an additional 3 min followed by 4 min of flotation. The yields of the concentrate and tailings were calculated after drying and weighing. Fig. S4 shows a flowchart of the microflotation test.

In this study, the recovery measurements are reported as the averages of three independent tests. The selectivity of NaOl in the tannin-pretreated magnesite–dolomite system was quantified using the selectivity index (SI), calculated as

$$\mathrm{SI} = \sqrt{\frac{R_m \times J_d}{(100 - R_m) \times (100 - J_d)}} \quad (1)$$

where J_d and R_m represent the recoveries of dolomite in the tailings and magnesite in the concentrate, respectively.

2.4. Contact angle measurements

The static contact angle of deionized water on each-mineral surface was measured using the suspension drop

method on a JC2000A contact angle measuring instrument [40]. The pretreated tannin ore sample and the pretreated sample prepared via the flotation test process were filtered and air dried at room temperature. The air-dried powdered ore sample was pressed into dense and smooth slices using a tablet press. The water was placed on a measuring platform and the liquid was dropped on its surface through a microsyringe. Liquid-wetting images of the mineral surface were collected to obtain the contact angle on the mineral surface. Each sample was tested in triplicate and the average was taken as the final result.

2.5. Zeta potential measurements

The zeta potentials of the mineral samples were measured under different pH conditions using a zeta potential analyzer (Malvern, UK) [41]. Prior to measurements, a 50-mg mineral sample (particle size less than 5 μm) was dispersed in 50 mL of KCl solution (10^{-3} mol/L) in a 50-mL beaker. The pH of the slurry was adjusted with HCl or NaOH solution for 3 min. The slurry was then stirred for 3 min and allowed to stand for 20 min. Furthermore, 1 mL of the upper suspension of each group was collected three times and the measurements were averaged to obtain the final result.

2.6. FT-IR tests

FT-IR spectra of the tannin-pretreated samples before and after NaOl treatment were obtained using an FT-IR spectrometer (Nicolet 460, Thermo Scientific, Waltham, Massachusetts, United States) in the range 400–4000 cm^{-1} [42]. The pretreated mineral samples and the NaOl-treated samples were air-dried at room temperature and ground to a particle size of <5 μm. A 2-mg portion of each sample was evenly mixed with 200 mg of spectral grade KBr (mass ratio 1:100) and pressed for measuring the FT-IR spectrum.

2.7. XPS detection

The chemical compositions of the magnesite and dolomite surface before and after tannin pretreatment (at pH 10.0) were measured under monochromatic Al Kα X-rays (1486.6 eV) generated by an ESCALAB 250Xi spectrometer (Thermo Scientific K-Alpha, USA) operated at 150 W [43]. The test samples were prepared following the flotation test process, washed thrice with deionized water, and dried for 24 h at <50°C. The binding energies were calibrated with the neutral C 1s carbon peak at 284.8 eV and the spectral results were processed using Thermo Avantage software.

2.8. DFT calculations

The crystal structures of magnesite and dolomite (see Fig. 1) were obtained from the Crystallography Open-Database.

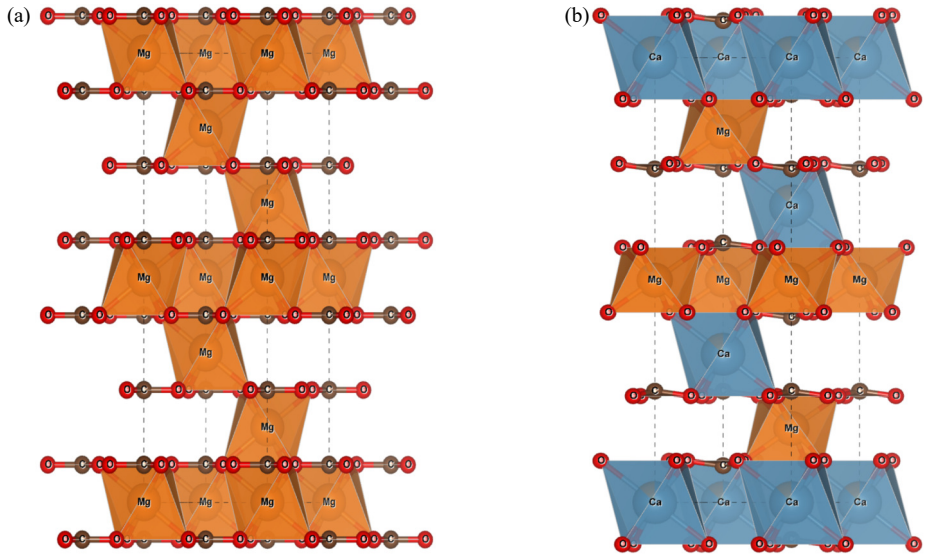

Fig. 1. Crystal structures of (a) magnesite and (b) dolomite.

The DFT calculations were performed on the Vienna *Ab-initio* Simulation Package. The long-range interactions arising from van der Waals forces were treated with the Perdew–Burke–Ernzerhof spin-polarized generalized gradient approximation [44]. To calculate the crystal properties and optimize the structural geometry, the Brillouin zone integration was adjusted by applying Monkhorst–Pack with *K*-point size of 5 × 5 × 1. The Gamma scheme with a *K*-point size of 1 × 1 × 1 was adopted for tannin. An original unit cell of magnesite or dolomite was constructed along the (104) direction. A minimum distance of 20 Å along the *z* direction was set as the vacuum layer. The plane wave was set with a cut-off energy of 400 eV and an energy convergence threshold of 10^{-5} eV.

At each ion-optimization step, the maximum Hellmann–Feynman force was 0.02 eV/Å. The oxygen adsorption energy (E_{ads}) was determined as

$$E_{ads} = E_{total} - (E_{mole} + E_{crystal}) \quad (2)$$

where E_{total} is the total energy of the adsorption structure, and E_{mole} and $E_{crystal}$ are the adsorption energies of tannin and the magnesite (or dolomite) crystal structure, respectively.

3. Results and discussion

3.1. Microflotation test

In the microflotation test, we measured the magnesite and dolomite flotation recoveries before and after tannin pretreatment for different NaOl dosages. The results are plotted in Fig. 2.

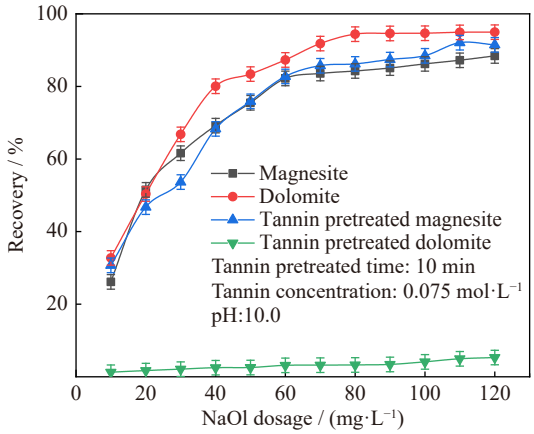

Fig. 2. Effect of NaOl dosage on the flotation recoveries of magnesite and dolomite before and after tannin pretreatment.

Increasing the NaOl dosage clearly increases the flotation recovery rates of the magnesite and dolomite single minerals, but the floatabilities of the two minerals are too close to achieve flotation separation. After tannin pretreatment in the NaOl system, the floatabilities of magnesite and dolomite are well separated because the pretreatment greatly reduces the dolomite floatability without affecting the magnesite floatability. The tannin pretreatment with 110 mg·L^{-1} NaOl maximizes the flotation recovery rate of magnesite at 92.05%, thereby achieving the maximum float difference (87.01%) between the two minerals after tannin pretreatment. Therefore, when exploring the effect of slurry pH on the floatabilities of magnesite and dolomite before and after pretreatment, the NaOl concentration was set to 110 mg·L^{-1}.

As the slurry pH increases, the flotation recovery rate of the magnesite and dolomite single minerals shows an overall upward trend but changing the slurry pH does not increase the small differences between the flotation recoveries of the two minerals (Fig. 3), so the flotation separation effect remains poor. After tannin pretreatment, the flotation recovery rate of magnesite first increases and then decreases while that of dolomite gradually decreases. The difference between the flotation recovery rates of the two minerals after tannin pretreatment becomes obvious in the pH range 9.0–11.0 and is maximized (86.65%) at pH 10.0. Therefore, when investigating the effect of pretreatment tannin concentration on the flotation recoveries of the two minerals, the pH was set to 10.0.

Changing the tannin concentration in the pretreatment agent little affects the flotation recovery rate of magnesite and dolomite (Fig. S5). This result indicates that the pretreatment can achieve the separation effect but the recovery rate is insensitive to tannin concentration. The floating difference

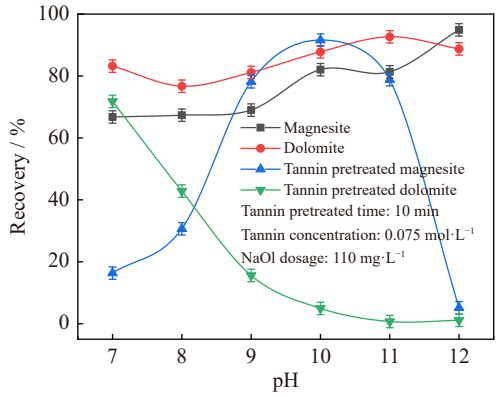

Fig. 3. Effect of pH on the flotation performances of magnesite and dolomite before and after tannin pretreatment.

was maximized (89.65%) at a tannin concentration of 0.075 mol·L^{-1}. Therefore, when investigating the influence of pretreatment time on the flotation separation of the two minerals, the tannin concentration was set to 0.075 mol·L^{-1}.

Fig. S6 shows the effect of tannin pretreatment time on the flotation separation performances of the two minerals. The plots are similar to those of tannin concentration. Notably, the pretreatment time exerts little influence on the pretreatment performance. The difference between the recovery rate of dolomite and magnesite was maximized (89.70%) at a pretreatment time of 10 min.

To further verify the sorting effect of the tannin pretreatment in the magnesite and dolomite single-mineral flotation tests, magnesite (1.6 g) and dolomite (0.4 g) before and after tannin pretreatment were subjected to a binary artificial mixed-ore test under the above determined optimal conditions. The results are shown in Table S2.

In the binary mixed ore with untreated magnesite and dolomite, the MgO and CaO grades in the concentrate were 42.18% and 5.78%, respectively, close to those in raw binary mixed ore. The low SI indicator (1.65) further indicates that the NaOl collector alone cannot separate magnesite from dolomite. In the binary mixed ore of magnesite and dolomite after the tannin pretreatment, the grade of MgO in the concentrate increased to 44.76% while the grade of CaO decreased to 2.84%. Meanwhile, the grade of CaO in the tailings increased from 6.10% to 16.21%, reflecting a significant decrease in the floatability of dolomite after pretreatment. The high SI (3.46) further indicates that the tannin pretreatment method selectively inhibits the flotation of dolomite, thus enhancing the flotation separation of the two minerals.

3.2. Contact angle analyses

The contact-angle characteristics of minerals directly reflect the wettability properties of flotation agents acting on the mineral surfaces. A mineral with a large contact angle will have high hydrophobicity and floatability [45–46]. The contact angles of magnesite and dolomite before and after applying the flotation agent are compared in Fig. 4.

The contact angles of magnesite and dolomite as single minerals were 25.86° and 27.03°, respectively (Fig. 4), increasing to 88.22° and 97.55° after treatment with NaOl, re-

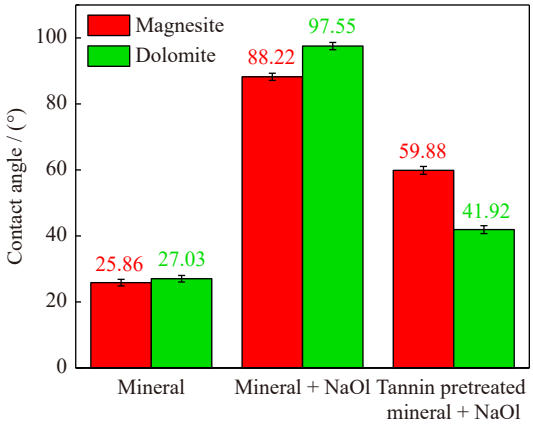

Fig. 4. Contact angles of magnesite and dolomite before and after flotation-agent action.

spectively. Notably, the values of the two minerals are considerably close, indicating similar floatabilities without tannin pretreatment. For magnesite and dolomite pretreated with tannin, their contact angles are 59.88° and 41.92°, respectively, which are 28.34° and 55.63° lower than those of magnesite and dolomite only treated with NaOl. This indicates that after tannin pretreatment, the floatability of dolomite decreases significantly, while the floatability of magnesite decreases less.

3.3. Zeta potential analysis

Zeta potential measurements analytically explain the flotation trends of different minerals exposed to different reagents [47–48]. Therefore, by measuring the zeta potentials under different pH conditions, we can understand the buoyancy characteristics of dolomite and magnesite mines. The pH dependences of the zeta potentials of dolomite and magnesite are shown in Figs. 5 and 6, respectively.

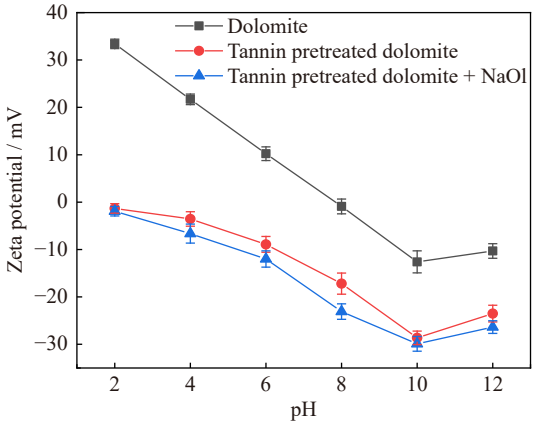

Fig. 5. Zeta potential versus pH of dolomite before and after flotation-agent action.

As the pH of the dolomite slurry increased, the zeta potential of dolomite generally decreased both before and after the action of the flotation agent (Fig. 5). After tannin pretreatment, the potentials became negative over the measured pH range. Under the flotation test condition (pH = 10.0), the zeta potential of dolomite changed from −12.60 to −28.64 mV. This large shift in zeta potential (−16.04 mV) indicates that

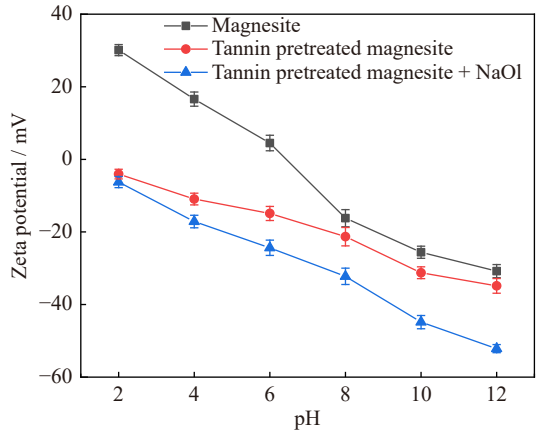

Fig. 6. Zeta potential versus pH of magnesite before and after the flotation-agent action.

the pretreated tannins are strongly adsorbed on the dolomite surface. The zeta potentials of dolomite after the addition of NaOl were similar to those without NaOl but were slightly shifted to more negative values. Under the flotation test condition (pH = 10.0), the zeta potential of dolomite changed from −28.64 to −29.91 mV, a decrease of 1.27 mV, indicating that NaOl is only weakly adsorbed on the dolomite surface after tannin pretreatment.

After tannin pretreatment, the zeta potentials of magnesite were shifted to negative values across the measured pH range (Fig. 6). Increasing the pH gradually increases the surface electronegativity of magnesite. Under the flotation test conditions (pH = 10.0), the zeta potential of magnesite decreased from −25.68 to −32.23 mV. This small shift in zeta potential (only −6.55 mV) indicates that the pretreated tannins are weakly adsorbed to the magnesite surface. In the presence of NaOl, the zeta potential of magnesite underwent a further negative shift and the offset increased more significantly under alkaline conditions. Under the flotation test condition (pH = 10.0), NaOl addition reduced the zeta potential of magnesite from −32.23 to −44.84 mV (a decrease of 12.61 mV). This large zeta potential offset indicates that NaOl strongly adsorbs to magnesite after the tannin pretreatment.

A comparison of the shifts in the zeta potentials of dolomite and magnesite after tannin pretreatment with NaOl showed that pretreatment with NaOl considerably enhances the adsorption capacity of magnesite. This result is attributable to strong adsorption of tannin on the dolomite surface, which hinders the adsorption of NaOl on dolomite. Conversely, as tannin adsorbs weakly to the magnesite surface, it does not affect the magnesite-acquisition ability of NaOl. Hence, the pretreatment method selectively reduces the floating ability of dolomite in the NaOl system by selectively blocking NaOl adsorption on the dolomite surface. This result is consistent with the contact-angle measurements.

3.4. FT-IR analysis

The contact-angle measurements and zeta potentials confirm that the tannin pretreatment method reduces the dolomite floatability without affecting the magnesite floatability. To fully explain the adsorption mechanism of NaOl on the

magnesite and dolomite surfaces after tannin pretreatment, the two minerals before and after treatment with the flotation reagent were analyzed using FT-IR. The FT-IR spectra of magnesite and dolomite are shown in Figs. 7 and 8, respectively.

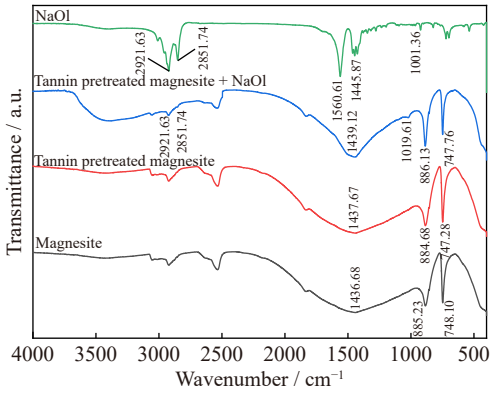

Fig. 7. FT-IR spectra of magnesite before and after the flotation-agent action. The spectrum of NaOl is also shown.

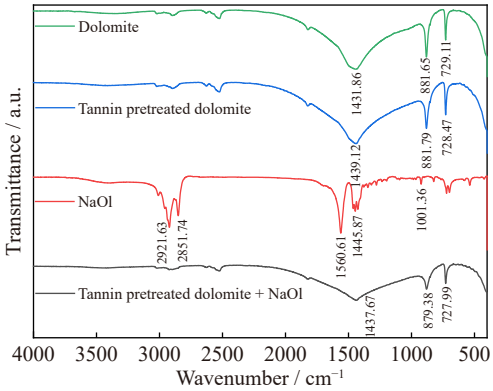

Fig. 8. FT-IR spectra of dolomite before and after the flotation-agent action. The spectrum of NaOl is also shown.

In the FTIR spectrum of NaOl (Fig. 7), the characteristic peaks at 1445.87 and 1560.61 cm^{-1} correspond to the symmetric and asymmetric vibration peak of –COO^-, respectively, and the characteristic peak at 1001.36 cm^{-1} is assigned to stretching vibrations of the C−O group [20,49]. The characteristic peaks at 2921.63 and 2851.74 cm^{-1} belong to stretching vibrations of $-CH_2$ and $-CH_3$, respectively [50–51].

The spectrum of the magnesite mono-mineral shows the peaks of C–O asymmetric telescopic vibrations peaks (1436.68 cm^{-1}) and C–O bending vibrations (885.23 and 748.10 cm^{-1}). After tannin pretreatment, these three magnesite peaks are shifted to 1437.67, 884.68, and 747.28 cm^{-1}, respectively. The small peak shifts (all within 2 cm^{-1}) reconfirm the weak adsorption capacity of the pretreatment tannins on the magnesite surface. NaOl treatment induced three new peaks at 2921.63, 2851.74, and 1019.61 cm^{-1}. These peaks are the characteristic peaks of NaOl, affirming that NaOl is indeed adsorbed on the surface of magnesite treated with tannin.

The FT-IR spectra of dolomite (Fig. 8) display three characteristic peaks of dolomite at 1431.86, 881.65, and 729.11 cm^{-1}. The first peak corresponds to asymmetric stretching vibrations of C–O and the latter two are assigned to bending vibrations of C–O. After tannin pretreatment, these characteristic dolomite peaks appeared at 1439.12, 881.79, and 728.47 cm^{-1}, respectively. Notably, the peak assigned to asymmetric C–O stretching vibrations peak shifted widely by 7.26 cm^{-1}, indicating that tannin is strongly adsorbed on the dolomite surface. In addition, NaOl application on the tannin-treated magnesite surface induced no new peaks of NaOl but reduced the intensity of the characteristic peaks of dolomite, indicating very weak adsorption of NaOl on the dolomite surface after tannin-treatment.

A comparison of Figs. 7 and 8 shows that NaOl can adsorb on the surface of tannin-treated magnesite but not on the surface of tannin-treated dolomite. Overall, the tannin pretreatment method selectively hinders the adsorption of NaOl on the dolomite surface. In other words, NaOl can selectively collect tannin-treated magnesite, thereby promoting the floating of magnesite and facilitating flotation separation of the two minerals.

3.5. XPS analysis

The abovementioned analysis shows that tannin pretreatment retains the floatability of magnesite but reduces the floatability of dolomite. However, the selective effect of tannic acid on the two minerals requires further exploration. Using XPS, this subsection evaluates the effect of tannin pretreatment on the surface elements and chemical compositions of magnesite and dolomite. The XPS spectra will help to reveal the interaction mechanism between tannin and magnesite or dolomite [52]. The atomic contents of the main elements on the magnesite and dolomite surfaces before and after tannin pretreatment are listed in Table S3.

After tannin pretreatment, the relative Mg content on the magnesite and dolomite surfaces decreased by 0.15at% and 0.11at%, respectively, and the relative Ca content on the dolomite surface decreased by 0.6at%, indicating a greater effect of tannin pretreatment on the Ca element than on the Mg element. As Ca and Mg are the characteristic elements of dolomite and magnesite, respectively, it was concluded that dolomite is more strongly influenced by tannin than magnesite.

To further explore how tannin influences the Mg and Ca elements of magnesite and dolomite, respectively, the Mg peak of magnesite and the Mg and Ca peaks of dolomite before and after tannin pretreatment were scrutinized by high-resolution scanning XPS. The results are shown in Figs. 9–11.

After tannin pretreatment, the Mg 1s peak of magnesite shifted from 1304.45 to 1304.47 eV (Fig. 9). This slight shift (0.02 eV) affirms that tannin pretreatment barely affects the chemical environment of the characteristic Mg elements on the magnesite surface. After tannin pretreatment, the Mg 1s peak of dolomite shifted from 1304.07 to 1304.05 eV (Fig. 10). This small shift in peak position (again only 0.02 eV) indicates that tannin pretreatment barely affects the chemical

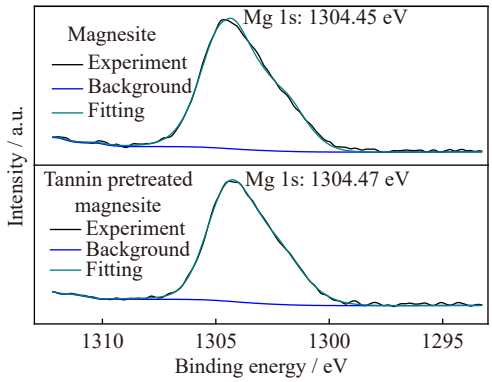

Fig. 9. X-ray photoelectron spectroscopy fitting peaks of Mg 1s on the magnesite surface before and after tannin pretreatment.

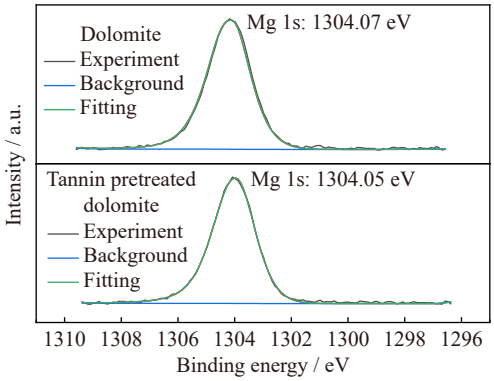

Fig. 10. X-ray photoelectron spectroscopy fitting peaks of Mg 1s on the dolomite surface before and after tannin pretreatment.

environment of the characteristic Mg elements on the dolomite surface.

After tannin pretreatment, the Ca 2p bimodal peak of dolomite shifted from 350.80 to 350.75 eV (Ca $2p_{1/2}$) and from 347.20 to 347.15 eV (Ca $2p_{3/2}$) (Fig. 11). The shift in the Ca 2p peak (0.05 eV) was 2.5 times larger than the shift in the Mg 1s peak of magnesite. Thus, tannin more strongly influences the Ca 2p peak than the Mg 1s peak, implying a strong relationship between tannin and the Ca elements on the dolomite surface. The results also prove that tannin is adsorbed on the dolomite surface through strong interactions with the Ca sites on dolomite, thus hindering the collection of NaOl on dolomite and inhibiting the floating of dolomite.

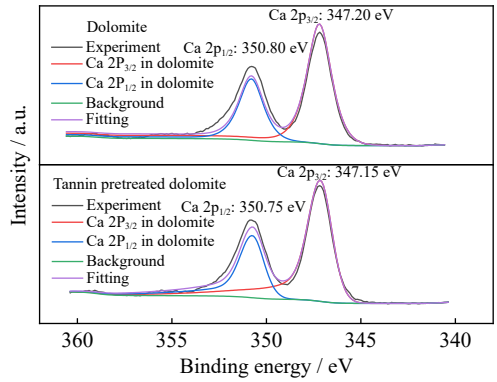

Fig. 11. X-ray photoelectron spectroscopy fitting peaks of Ca 2p on the dolomite surface before and after tannin pretreatment.

3.6. DFT analysis

As demonstrated in many related studies, the surface properties of minerals are largely determined by the characteristics of their most commonly exposed surfaces. XRD results show that the (104) surfaces of magnesite and dolomite are most commonly exposed during the crushing process [34]. To further explore the selective properties of the tannin pretreatment on the mineral surfaces, the interactions between small tannin molecules and the magnesite (104) and dolomite (104) surfaces were simulated through DFT calculations. The simulation results are shown in Fig. 12.

When small tannin molecules interact with the magnesite surface, the Mg–O bond length is 4.89 Å, but when the tannin molecules interact with dolomite, the Ca–O bond length is 3.91 Å. The Mg–O bond is longer than the Ca–O bond, indicating that tannin interactions are weaker at the Mg sites than at the Ca sites. Additionally, the adsorption capacities of flotation agents on mineral surfaces can be determined from their characteristic interaction energies on the surfaces. Generally, the lower the interaction energy, the more closely the flotation agent interacts with the mineral surface. Moreover, the structure becomes more stable as its binding strength increases [53]. The simulated tannin–magnesite and tannin–dolomite interaction energies are shown in Table S4.

The tannin–magnesite (104) and tannin–dolomite (104) interaction energies are −0.817033 and −5.218543 eV, respectively. As the interaction energies are negative, the tan-

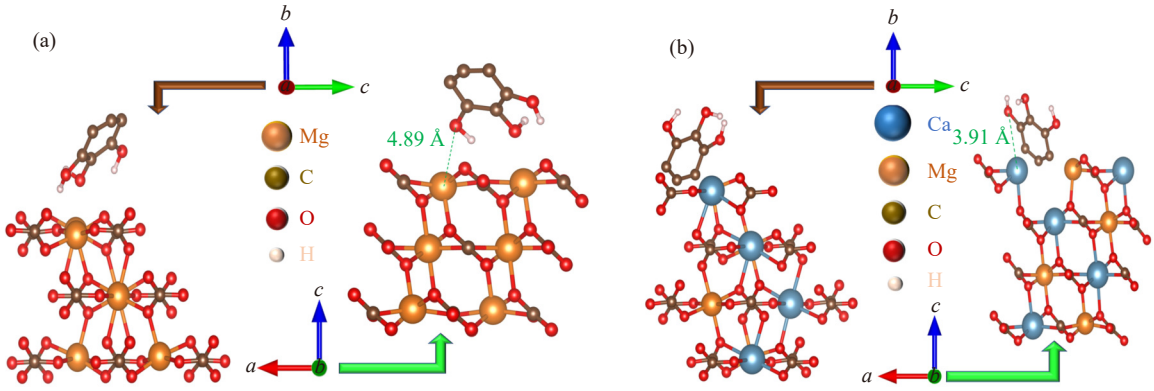

Fig. 12. Small tannin molecules interacting with the mineral surfaces in the (a) magnesite and (b) dolomite models.

nin molecules spontaneously adsorb to magnesite and dolomite [54]. The negative interaction energy between tannin and dolomite exceeds that between tannin and magnesite by more than six times, implying that tannin more easily combines with dolomite than with magnesite in the same environment. This result is consistent with the XPS analysis above.

3.7. Analysis of flotation-separation causes in the tannin pretreatment method

Fig. 13 illustrates the mechanism of the tannin pretreatment method for the flotation separation of magnesite and dolomite. This diagram was deduced from the flotation test results and detection results. In the proposed model, when the pretreated tannins fully contact the magnesite and dolomite surfaces, the difference between the adsorption capacities on the two surfaces increases. Considering the measurement results of the contact angle, the adsorption of tannin on the dolomite surface reduces the floatability of dolomite and interferes with the collection ability of NaOl. According to the zeta potential and FT-IR analyses, NaOl is better adsorbed on the magnesite surface than on the dolomite surface. The XPS analysis and DFT simulations further verified the strong selective adsorption between tannin and dolomite and the strong affinity of tannin for Ca sites. The tannin pretreatment method clearly achieves the flotation separation of magnesite and dolomite by hindering the adsorption of the NaOl collector on the surface of pretreated dolomite.

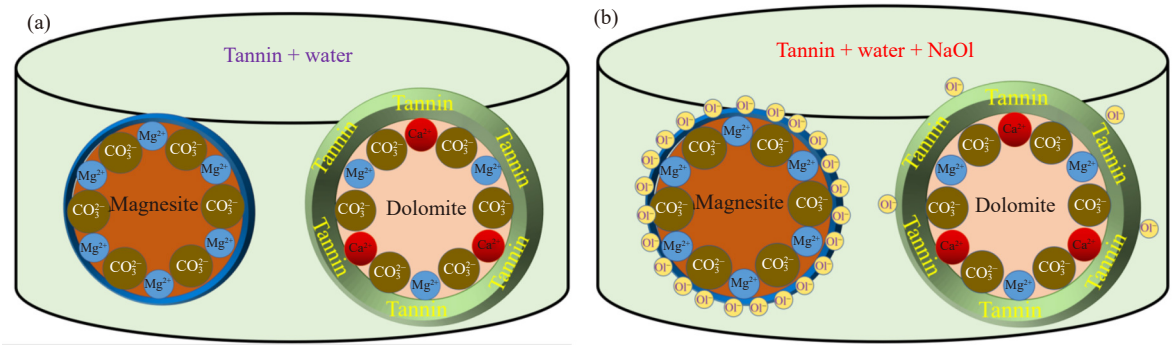

Fig. 13. Possible adsorption model of flotation separation of magnesite from dolomite by tannin pretreatment.

4. Conclusions

This study achieved the flotation separation of magnesite and dolomite via tannin pretreatment in the NaOl system prior to the flotation test. Based on contact angle measurements, zeta potential measurements, and FT-IR analyses, the underlying mechanism of flotation separation via tannin pretreatment was analyzed. Furthermore, XPS detection and DFT calculations characterized the tannin interactions on the two minerals. The main conclusions are summarized below.

(1) The tannin pretreatment method enables high-efficiency flotation separation of magnesite and dolomite. Pretreatment with tannin considerably reduces the dolomite floatability under the NaOl system, but it does not affect magnesite floatability.

(2) The strong adsorption of tannin on the dolomite surface hinders the harvesting of dolomite by NaOl but not that of magnesite. The strong adsorption of tannin on the dolomite surface is attributed to the stronger binding ability to Ca sites on the dolomite surface than to other sites.

(3) When tannin is spontaneously adsorbed on the surface of magnesite and dolomite, it preferentially bonds to dolomite because tannin–dolomite bonding has a lower interaction energy than tannin–magnesite bonding.

Acknowledgements

This work was financially supported by the National Natural Science Foundation of China (Nos. 51974064, 52174239, and 52374259) and the Open Project of the Key Laboratory of Solid Waste Treatment and Resource Utilization of the Ministry of Education, China (No. 23kfgk02). We are also grateful for the support of Scientific Compass in conducting the DFT simulations and improving the language of the article.

Conflict of Interest

Wanzhong Yin is an editorial board member for this journal and not involved in the editorial review or the decision to publish this article. All authors declare that there is no conflict of interest regarding the publication of this paper.

Supplementary Information

The online version contains supplementary material at https://doi.org/10.1007/s12613-023-2708-4.

References

[1] C.L. Adam, R.G. Hemingway, and N.S. Ritchie, Influence of manufacturing conditions on the bioavailability of magnesium in calcined magnesites measured *in vivo* and *in vitro*, *J. Agric. Sci.*, 127(1996), No. 3, p. 377.

[2] C. Aksel, F. Kasap, and A. Sesver, Investigation of parameters affecting grain growth of sintered magnesite refractories, *Ceram. Int.*, 31(2005), No. 1, p. 121.

[3] S.M. Aleksandrov and V.G. Senin, Genesis, composition, and evolution of sulfide mineralization in magnesian skarns, *Geo-*

chem. Int., 43(2005), No. 6, p. 559.
[4] M. Guo, Q. Li, H.N. Liu, *et al*., The exploitation and utilization of magnesium resources in salt lakes, *Prog. Chem.*, 21(2009), No. 11, p. 2358.
[5] J.Z. Cai, J.S. Deng, L. Wang, *et al*., Reagent types and action mechanisms in ilmenite flotation: A review, *Int. J. Miner. Metall. Mater.*, 29(2022), No. 9, p. 1656.
[6] D. Wonyen, V. Kromah, B. Gibson, S. Nah, and S. Chelgani, A review of flotation separation of Mg carbonates (dolomite and magnesite), *Minerals*, 8(2018), No. 8, art. No. 354.
[7] Z.Y. Chang, S.S. Niu, Z.C. Shen, L.C. Zou, and H.J. Wang, Latest advances and progress in the microbubble flotation of fine minerals: Microbubble preparation, equipment, and applications, *Int. J. Miner. Metall. Mater.*, 30(2023), No. 7, p. 1244.
[8] Z.L. Zhu, Y.F. Fu, W.Z. Yin, *et al*., Role of surface roughness in the magnesite flotation and its mechanism, *Particuology*, 62(2022), p. 63.
[9] H.R. Sun, F. Han, W.Z. Yin, J. Hong, and B. Yang, Modification of selectivity in the flotation separation of magnesite from dolomite, *Colloids Surf. A: Physicochem. Eng. Aspects*, 606(2020), art. No. 125460.
[10] Y.F. Fu, Y. Hou, R. Wang, *et al*., Detailed insights into improved chlorite removal during hematite reverse flotation by sodium alginate, *Miner. Eng.*, 173(2021), art. No. 107191.
[11] M.Y. Li, C. Yang, Z.Y. Wu, *et al*., Selective depression action of taurine in flotation separation of specularite and chlorite, *Int. J. Min. Sci. Technol.*, 32(2022), No. 3, p. 637.
[12] B. Feng, L.Z. Zhang, W.P. Zhang, H.H. Wang, and Z.Y. Gao, Mechanism of calcium lignosulfonate in apatite and dolomite flotation system, *Int. J. Miner. Metall. Mater.*, 29(2022), No. 9, p. 1697.
[13] A. Bastrzyk, I. Polowczyk, Z. Sadowski, and A. Sikora, Relationship between properties of oil/water emulsion and agglomeration of carbonate minerals, *Sep. Purif. Technol.*, 77(2011), No. 3, p. 325.
[14] Q. Dehaine, L.O. Filippov, I.V. Filippova, L.T. Tijsseling, and H.J. Glass, Novel approach for processing complex carbonate-rich copper–cobalt mixed ores via reverse flotation, *Miner. Eng.*, 161(2021), art. No. 106710.
[15] D. Li, W.Z. Yin, J.W. Xue, J. Yao, Y.F. Fu, and Q. Liu, Solution chemistry of carbonate minerals and its effects on the flotation of hematite with sodium oleate, *Int. J. Miner. Metall. Mater.*, 24(2017), No. 7, p. 736.
[16] X. Liu, C.X. Li, H.H. Luo, R.J. Cheng, and F.Y. Liu, Selective reverse flotation of apatite from dolomite in collophanite ore using saponified gutter oil fatty acid as a collector, *Int. J. Miner. Process.*, 165(2017), p. 20.
[17] M.P. Majewska, R. Miltko, G. Bełżecki, A. Kędzierska, and B. Kowalik, Comparison of the effect of synthetic (tannic acid) or natural (oak bark extract) hydrolysable tannins addition on fatty acid profile in the rumen of sheep, *Animals*, 12(2022), No. 6, art. No. 699.
[18] J. Yao, H.R. Sun, X.Q. Ban, and W.Z. Yin, Analysis of selective modification of sodium dihydrogen phosphate on surfaces of magnesite and dolomite: Reverse flotation separation, adsorption mechanism, and density functional theory calculations, *Colloids Surf. A: Physicochem. Eng. Aspects*, 618(2021), art. No. 126448.
[19] W.Z. Yin, H.R. Sun, J. Hong, *et al*., Effect of Ca selective chelator BAPTA as depressant on flotation separation of magnesite from dolomite, *Miner. Eng.*, 144(2019), art. No. 106050.
[20] J. Yao, B. Yang, K.Q. Chen, *et al*., Sodium tripolyphosphate as a selective depressant for separating magnesite from dolomite and its depression mechanism, *Powder Technol.*, 382(2021), p. 244.
[21] Y.G. Zhu, L.F. Yang, X.X. Hu, X.R. Zhang, and G.B. Zheng, Flotation separation of quartz from magnesite using carboxymethyl cellulose as depressant, *Trans. Nonferrous Met. Soc. China*, 32(2022), No. 5, p. 1623.
[22] H. Han, A. Liu, C.L. Wang, R.Q. Yang, S. Li, and H.F. Wang, Flotation kinetics performance of different coal size fractions with nanobubbles, *Int. J. Miner. Metall. Mater.*, 29(2022), No. 8, p. 1502.
[23] H.R. Sun, B. Yang, Z.L. Zhu, *et al*., New insights into selective-depression mechanism of novel depressant EDTMPS on magnesite and quartz surfaces: Adsorption mechanism, DFT calculations, and adsorption model, *Miner. Eng.*, 160(2021), art. No. 106660.
[24] B. Yang, D.H. Wang, S.H. Cao, *et al*., Selective adsorption of a high-performance depressant onto dolomite causing effective flotation separation of magnesite from dolomite, *J. Colloid Interface Sci.*, 578(2020), p. 290.
[25] C.H. Zhang, S. Wei, Y.H. Hu, *et al*., Selective adsorption of tannic acid on calcite and implications for separation of fluorite minerals, *J. Colloid Interface Sci.*, 512(2018), p. 55.
[26] G.L. Chen and D. Tao, Reverse flotation of magnesite by dodecyl phosphate from dolomite in the presence of sodium silicate, *Sep. Sci. Technol.*, 39(2005), No. 2, p. 377.
[27] W.B. Liu, W.X. Huang, F. Rao, Z.L. Zhu, Y.M. Zheng, and S.M. Wen, Utilization of DTAB as a collector for the reverse flotation separation of quartz from fluorapatite, *Int. J. Miner. Metall. Mater.*, 29(2022), No. 3, p. 446.
[28] G.A. Oliveira, Ê.L. Machado, R.S. Knoll, N. Dell'Osbel, G.S. Colares, and L.R. Rodrigues, Combined system for wastewater treatment: Ozonization and coagulation via tannin-based agent for harvesting microalgae by dissolved air flotation, *Environ. Technol.*, 43(2022), No. 9, p. 1370.
[29] M. Murugananthan, G. Bhaskar Raju, and S. Prabhakar, Removal of tannins and polyhydroxy phenols by electro-chemical techniques, *J. Chem. Technol. Biotechnol.*, 80(2005), No. 10, p. 1188.
[30] J.H. Chen, Y.Q. Li, Q.R. Long, Z.W. Wei, and Y. Chen, Improving the selective flotation of jamesonite using tannin extract, *Int. J. Miner. Process.*, 100(2011), No. 1-2, p. 54.
[31] P.E. Sarquís, J.M. Menéndez-Aguado, M.M. Mahamud, and R. Dzioba, Tannins: The organic depressants alternative in selective flotation of sulfides, *J. Clean. Prod.*, 84(2014), p. 723.
[32] Z.H. Shen, S.M. Wen, H. Wang, *et al*., Effect of dissolved components of malachite and calcite on surface properties and flotation behavior, *Int. J. Miner. Metall. Mater.*, 30(2023), No. 7, p. 1297.
[33] J. Yao, H.R. Sun, F. Han, *et al*., Enhancing selectivity of modifier on magnesite and dolomite surfaces by pH control, *Powder Technol.*, 362(2020), p. 698.
[34] B. Yang, H.R. Sun, D.H. Wang, *et al*., Selective adsorption of a new depressant Na_2ATP on dolomite: Implications for effective separation of magnesite from dolomite via froth flotation, *Sep. Purif. Technol.*, 250(2020), art. No. 117278.
[35] E. Gülcan and Ö.Y. Gülsoy, Performance evaluation of optical sorting in mineral processing—A case study with quartz, magnesite, hematite, lignite, copper and gold ores, *Int. J. Miner. Process.*, 169(2017), p. 129.
[36] H. Yilmaz Atay and M. Çirak, Separation of huntite and hydromagnesite from magnesite in combination of physicochemical treatment and size reduction, *Ain Shams Eng. J.*, 10(2019), No. 1, p. 113.
[37] L.L. Godirilwe, R.S. Magwaneng, R. Sagami, *et al*., Extraction of copper from complex carbonaceous sulfide ore by direct high-pressure leaching, *Miner. Eng.*, 173(2021), art. No. 107181.
[38] T.C. Wang, G.J. Sun, J.S. Deng, *et al*., A depressant for marmatite flotation: Synthesis, characterisation and floatation performance, *Int. J. Miner. Metall. Mater.*, 30(2023), No. 6, p. 1048.

[39] X.F. Gong, J. Yao, B. Yang, J. Guo, H.R. Sun, and W.Z. Yin, Study on the inhibition mechanism of guar gum in the flotation separation of brucite and dolomite in the presence of SDS, *J. Mol. Liq.*, 380(2023), art. No. 121721.

[40] J.W. Xue, H.Z. Tu, J. Shi, Y.N. An, H. Wan, and X.Z. Bu, Enhanced inhibition of talc flotation using acidified sodium silicate and sodium carboxymethyl cellulose as the combined inhibitor, *Int. J. Miner. Metall. Mater.*, 30(2023), No. 7, p. 1310.

[41] L.P. Luo, L.H. Xu, X.Z. Shi, J.P. Meng, and R.H. Liu, Micro-scale insights into the influence of grinding media on spodumene micro-flotation using mixed anionic/cationic collectors, *Int. J. Min. Sci. Technol.*, 32(2022), No. 1, p. 171.

[42] X.F. Gong, J. Yao, B. Yang, *et al*., Activation–inhibition mechanism of diammonium hydrogen phosphate in flotation separation of brucite and calcite, *J. Environ. Chem. Eng.*, 11(2023), No. 3, art. No. 110184.

[43] Z.X. Wu, D.P. Tao, Y.J. Tao, M. Jiang, and P. Zhang, A novel cationic collector for silicon removal from collophane using reverse flotation under acidic conditions, *Int. J. Miner. Metall. Mater.*, 30(2023), No. 6, p. 1038.

[44] F.Y. Ma, P. Zhang, and D.P. Tao, Surface nanobubble characterization and its enhancement mechanisms for fine-particle flotation: A review, *Int. J. Miner. Metall. Mater.*, 29(2022), No. 4, p. 727.

[45] N. Gence, Wetting behavior of magnesite and dolomite surfaces, *Appl. Surf. Sci.*, 252(2006), No. 10, p. 3744.

[46] B. Yang, W.Z. Yin, Z.L. Zhu, *et al*., Differential adsorption of hydrolytic polymaleic anhydride as an eco-friendly depressant for the selective flotation of apatite from dolomite, *Sep. Purif. Technol.*, 256(2021), art. No. 117803.

[47] Y.H. Wang, N. Sun, H.R. Chu, X.Y. Zheng, D.F. Lu, and H.T. Zheng, Surface dissolution behavior and its influences on the flotation separation of spodumene from silicates, *Sep. Sci. Technol.*, 56(2021), No. 8, p. 1407.

[48] B. Yang, Z.L. Zhu, H.R. Sun, *et al*., Improving flotation separation of apatite from dolomite using PAMS as a novel eco-friendly depressant, *Miner. Eng.*, 156(2020), art. No. 106492.

[49] W.Z. Yin, B. Yang, Y.F. Fu, *et al*., Effect of calcium hypochlorite on flotation separation of covellite and pyrite, *Powder Technol.*, 343(2019), p. 578.

[50] R.Q. Xie, X. Tong, X. Xie, Y.M. Zhu, and J. Liu, Flaxseed gum as new depressant in the separation of apatite and dolomite and its mechanism, *Appl. Surf. Sci.*, 593(2022), art. No. 153390.

[51] J. Yao, X.F. Gong, H.R. Sun, R.F. He, and W.Z. Yin, Separation of magnesite and calcite based on flotation solution chemistry, *Physicochem. Probl. Miner. Process.*, 58(2022), No. 4, art. No. 149398.

[52] J.J. Wang, W.H. Li, Z.H. Zhou, Z.Y. Gao, Y.H. Hu, and W. Sun, 1-Hydroxyethylidene-1,1-diphosphonic acid used as pH-dependent switch to depress and activate fluorite flotation I: Depressing behavior and mechanism, *Chem. Eng. Sci.*, 214(2020), art. No. 115369.

[53] Y. Tang, H.R. Sun, W.Z. Yin, *et al*., Computational modeling of cetyl phosphate adsorption on magnesite (104) surface, *Miner. Eng.*, 171(2021), art. No. 107123.

[54] Y. Tang, W.Z. Yin, and S. Kelebek, Molecular dynamics simulation of magnesite and dolomite in relation to flotation with cetyl phosphate, *Colloids Surf. A*: *Physicochem. Eng. Aspects*, 610(2021), art. No. 125928.